Auxin activity and molecular structure of 2-alkylindole-3-acetic acids

Antolic, Snjezana; Dolusic, Eduard; Kozic, Erika K.; Kojic-Prodic, Biserka; Magnus, Volker; Ramek, Michael; Tomic, Sanja

Published in:
Plant Growth Regulation

DOI:
10.1023/A:1022894914226

Publication date:
2003

Document Version
Publisher's PDF, also known as Version of record

Plant Growth Regulation **39:** 235–252, 2003.

Auxin activity and molecular structure of 2-alkylindole-3-acetic acids

Snježana Antolić[1], Eduard Dolušić[1], Erika K. Kožić[1], Biserka Kojić-Prodić[1], Volker Magnus[1,*], Michael Ramek[2] and Sanja Tomić[1]

*[1]Ruđer Bošković Institute, Bijenička cesta 54, p. p. 180, HR-10002 Zagreb, Croatia; [2]Institut für physikalische und theoretische Chemie, Technische Universität Graz, A-8010 Graz, Austria; *Author for correspondence (e-mail: magnus@rudjer.irb.hr; phone: +385-1-4561-002; fax: +385-1-4561-177)*

Received 12 March 2002; accepted in revised form 19 August 2002

Key words: 2-Ethylindole-3-acetic acid, 2-Propylindole-3-acetic acid, Auxin, Conformational analysis, Indole-3-acetic acid, X-ray crystallography

Abstract

2-Methylindole-3-acetic acid (2-Me-IAA) is a known auxin, but its 2-ethyl homologue has been considered inactive. Here we show that the compound previously bioassayed as '2-ethylindole-3-acetic acid' (2-Et-IAA) was, in fact, 3-(3-methylindol-2-yl)propionic acid. The proper 2-Et-IAA and its 2-(*n*-propyl) homologue (2-Pr-IAA) are prepared, unambiguously characterized, and their auxin activity is demonstrated in the *Avena* coleoptile-section straight-growth test. Their half-optimal concentrations are approximately the same as for 2-Me-IAA (2×10^{-5} mol L^{-1}), and hence about ten times larger than for unsubstituted indole-3-acetic acid (IAA) and its derivatives alkylated in positions 4, 5, 6 or 7. The optimal response elicited by 2-Et-IAA and 2-Pr-IAA is about half that observed for 2-Me-IAA. These characteristics place the three 2-alkyl-IAAs along the borderline between the classes of strong and weak auxins, thus corroborating the results of *interaction similarity analysis*, a mathematical approach based on the capability of auxin molecules to participate in non-bonding interactions with a generalized receptor protein. X-ray diffraction analysis shows no explicit structural features to be blamed for the decrease in auxin activity caused by attaching a 2-alkyl substituent to the IAA molecule; sterical interference of the 3-CH_2COOH group and the 2-alkyl moiety is barely recognizable in the crystalline state. Quantum-chemical calculations and molecular dynamics simulations suggest that 2-alkyl-IAAs, in the absence of crystal-packing restraints, prefer conformations with the CH_2-COOH bond tilted to the heterocyclic ring system. Substantially higher conformational energy (and hence lower abundance) is predicted for planar conformers which were previously shown to prevail for IAA and many of its derivatives substituted in the benzene moiety of the indole nucleus. This shift in the rotational preferences of the -CH_2COOH moiety may be one of the reasons for the reduced plant-growth promoting activity of 2-alkyl-IAAs.

Abbreviations: 2-Et-IAA – 2-ethylindole-3-acetic acid, 2-Pr-IAA – 2-(*n*-propyl)indole-3-acetic acid, IAA – indole-3-acetic acid, TLC – thin-layer chromatography

Introduction

A large number of indole-3-acetic acids (IAAs) substituted in the side chain and in ring-positions 4–7 have been screened for their plant-growth regulating properties (Antolić et al. 1996, 1999; Hatano et al. 1987; Jönsson 1961; Katayama et al. 1998; Katekar 1979; Kojić-Prodić et al. 1991; Nigović et al. 2000; Porter and Thimann 1965), but derivatives with substituents in the (pyrrole) 2-position have received little attention. Yet, these IAA derivatives are of theoretical interest because large 2-substituents may block access to the carboxyl group, a structural element which appears to be critical for recognition by proteins which participate in auxin physiology.

2-Methylindole-3-acetic acid (2-Me-IAA; Figure 1) is somewhat less active than IAA in a variety of bioassays (Hoffmann et al. 1952; Kögl and Kostermans 1935; Muir et al. 1949; Muir and Hansch 1953; Nigović et al. 2000; Porter and Thimann 1965; Rescher et al. 1996; Sell et al. 1952). Adding a 2-methyl group to 5-chloro-IAA, 7-chloro-IAA, 4,7-dichloro-IAA and 5,7-dichloro-IAA also reduces auxin activity (Hoffmann et al. 1952; Muir et al. 1949). On the other hand, there have only been few attempts to introduce substituents other than methyl into the IAA 2-position. Kögl and Kostermans (1935) allegedly prepared 2-ethylindole-3-acetic acid (2-Et-IAA) and found no growth-promoting activity, but could not, in 1935, establish the chemical identity of their product beyond reasonable doubt. In fact, Walton et al. (1968) attributed the same structure to a compound with a melting point about 100° above that reported by Kögl and Kostermans (1935). Porter and Thimann (1965) synthesized 2-chloroindole-3-acetic and 2-bromoindole-3-acetic acids, both of which were claimed to be more active than IAA in the split pea-stem curvature bioassay. Unfortunately, the C2-halogen bond is subject to acid-catalyzed hydrolysis (Porter and Thimann 1965; Lawson et al. 1960) and the hydrochloric and hydrobromic acids thus formed not only accelerate the decomposition, but may also cause an acid-growth response (Cosgrove 1998).

Here we demonstrate that the compound Kögl and Kostermans (1935) described as '2-Et-IAA' was, in fact, its isomer, 3-(3-methylindol-2-yl)propionic acid which is not expected to be an auxin. Authentic 2-Et-IAA and its homologue, 2-(*n*-propyl)indole-3-acetic acid (2-Pr-IAA) are prepared by an unequivocal route, characterized by spectroscopic and crystallographic methods, and shown to be auxins. Their plant-growth promoting properties are rationalized considering their molecular structures in the solid state and in solution. Interaction similarity analysis also suggests that the two 2-alkyl-IAAs fit well into the auxin family.

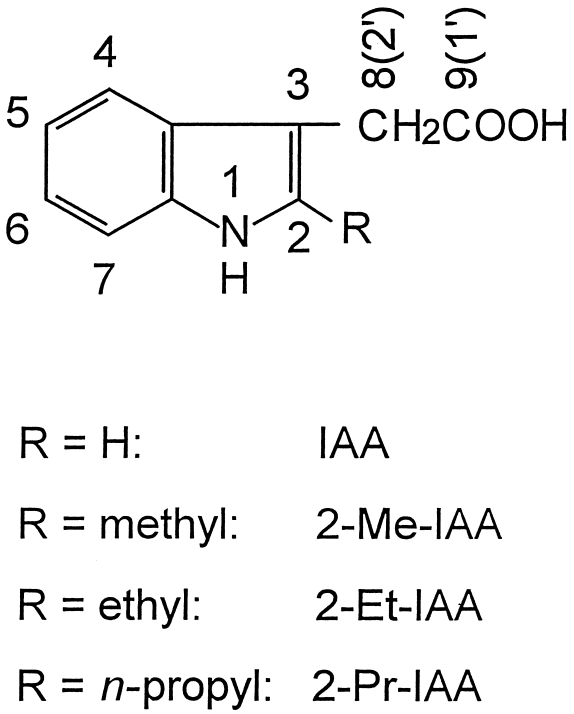

Figure 1. Structural formulae of the auxins studied indicating the numbering of selected positions. For the 3-side chain, the crystallographic numbering conventions used in this report differ from IUPAC recommendations (shown in parentheses).

Materials and methods

Bioassays

Auxin activity was monitored by the *Avena* coleoptile-section straight-growth test (Mitchell and Livingston 1968; Larsen 1961). In brief, seeds of *Avena sativa* L. cv. Pula and cv. Valiant were soaked in running tap water for 6 h, sown onto moist vermiculite, and germinated at 27 °C, for ca. 80 h, in complete darkness, except for a short daily exposure to red light. Coleoptiles, 25–30 mm in length, were selected under green light and 10 mm sections (1 per coleoptile) were excised starting 2 mm below the tip. They were temporarily (ca. 2 h) stored floating on distilled water before being distributed, in aliquots of 10–15, to disposable polystyrene Petri dishes (diameter: 3 cm) containing 2.7 mL of auxin solution in glass-distilled water. A water control and a complete series of IAA dilutions were included in each set of bioassays. After 20 h of growth in darkness at 27 °C, shadow graphs (original size) of the sections on photographic paper were prepared and measured to the nearest 0.1 mm. To the dose-response data were fitted fourth- and fifth-degree polynomials and the function

$$y = d + (a/s)[1/(x + c)]\exp\{ - [\ln(x + c) - b]^2/2s^2\}$$

wherein y is the length of the coleoptile sections in mm, x is the negative logarithm of the auxin concentration in mol L^{-1}, and a, b, c, d and s are shape parameters optimized by the fitting process. The curve

optimally representing the data points was chosen to estimate the maximal elongation and the optimal and half-optimal concentrations.

Preparative methods

General

Melting points were determined in open capillaries and were not corrected. UV spectra were measured using a Varian Cary 5 digital spectrophotometer. NMR spectra were recorded at 20 °C on a Varian Gemini 300 spectrometer operating at 300 MHz for ^{1}H and at 75 MHz for ^{13}C. Chemical shifts are reported in parts per million downfield from tetramethylsilane. Column chromatography was on silica gel 60 (Merck), particle diameter: 0.063–0.2 mm. Thin-layer chromatography (TLC) was on silica gel GF_{254} (Merck) developing with dichloromethane/methanol/acetic acid (90:10:1, solvent A_1; 100:50:2, solvent A_2; 90:45:5, solvent A_3; 100:20:5, solvent A_4; 90:5:1, solvent A_5), 2-propanol/ethyl acetate/25% aq. ammonia (35:45:20; solvent B), and 2-propanol/ethyl acetate/water (24:65:11, solvent C). In addition to detection by UV absorption, chromatograms were sprayed with the Ehrlich reagent (1% *p*-dimethylaminobenzaldehyde in a 1/1 mixture of ethanol and 35% HCl). The solvents employed were of analytical purity; the use of phosgene-free chloroform (stabilized with 1% ethanol) and peroxide-free diethyl ether and dioxane is essential. 4-ketohexanoic (homolevulinic) acid was obtained as follows: methyl 4-nitrohexanoate was prepared by triethylamine-catalyzed condensation of 1-nitropropane and methyl acrylate (Kloetzel 1948), purified by column chromatography (eluent dichloromethane containing decreasing proportions of *n*-heptane), and its sodium salt (prepared in 20% v/v aq. EtOH) was subjected to acid decomposition (Nef reaction) (Kloetzel 1948). 2-Ethylindole and 2-(*n*-propyl)indole were synthesized by sodium amide-mediated cyclization of *N*-propyl and *N*-butyl-*o*-toluidine (Verley and Beduwé 1925). All other chemicals used, including 2-Me-IAA, were obtained through commercial suppliers. The essential steps in the syntheses performed herein are summarized in Figure 2.

2-Ethylgramine
[N,N-dimethyl-(2-ethylindole-3-)methanamine]

2-Ethylindole was treated with formaldehyde/dimethylamine in dioxane/acetic acid, essentially as described by Le Goffic et al. (1973), except that the product was recrystallized from acetone/cyclohexane (1:9). M. p. 115–117 °C [lit. (Le Goffic et al. 1973) 119–121 °C; from acetone/water]. R_f = 0.7 (solvent A_2), 0.6 (solvent A_3), 0.7 (solvent B). *^{1}H-NMR (CD_3OD).* Gramine moiety: δ7.60 (dd, 1H, $J_{4,5}$ = 6.8 Hz, $J_{4,6}$ = 1.4 Hz, H-4), 7.06 (ddd, 1H, $J_{5,6}$ = 7.2 Hz, $J_{5,7}$ = 1.2 Hz, H-5), 7.11 (ddd, 1H, H-6), 7.35 (dd, 1H, $J_{6,7}$ = 7.1 Hz, H-7), 3.68 (s, 2H, CH_2), 2.34 (s, 6H, $2CH_3$); ethyl moiety: δ2.90 (q, 2H, J_{vic} = 7.6 Hz, CH_2), 1.40 (t, 3H, CH_3). *^{13}C-NMR (CD_3OD).* Gramine moiety: δ141.7 (C-2), 107.0 (C-3), 130.6 (C-3a), 120.1, 119.4 (C-4, C-6), 121.9 (C-5), 111.7 (C-7), 137.4 (C-7a), 53.8 (CH_2), 45.5 ($2CH_3$); ethyl moiety: δ20.5 (α-C), 14.7 (β-C).

*2-(*n*-Propyl)gramine*
*[N,N-dimethyl-(2-*n*-propylindole-3-)methanamine]*

2-(*n*-Propyl)indole, when processed as described for the preparation of 2-ethylgramine, afforded 74% of the title compound, m. p. 98 – 100 °C, R_f = 0.8 (solvent A_2), 0.4 (solvent A_4), 0.8 (solvent B). *^{1}H-NMR (CD_3OD).* Gramine moiety: δ7.51 (ddd, 1H, $J_{4,5}$ = 7.3 Hz, $J_{4,7}$ = 1.0 Hz, H-4), 6.97 (ddd, 1H, $J_{5,6}$ = 7.0 Hz, $J_{5,7}$ = 1.2 Hz, H-5), 7.02 (ddd, 1H, $J_{4,6}$ = 1.5 Hz, H-6), 7.25 (dd, 1H, $J_{6,7}$ = 7.1 Hz, H-7), 3.59 (s, 2H, CH_2), 2.25 (s, 6H, $2CH_3$); *n*-propyl moiety: δ2.76 (t, 2H, J_{vic} = 7.6 Hz, α-CH_2), 1.74 (sextet, 2H, β-CH_2), 0.97 (t, 3H, J_{vic} = 7.4 Hz, CH_3). *^{13}C-NMR (CD_3OD).* Gramine moiety: δ140.2 (C-2), 107.8 (C-3), 130.5 (C-3a), 120.0, 119.4 (C-4, C-6), 121.9 (C-5), 111.7 (C-7), 137.4 (C-7a), 53.9 (CH_2), 45.6 ($2CH_3$); *n*-propyl moiety: 29.4 (α-C), 24.3 (β-C), 14.6 (CH_3).

2-Ethylindole-3-acetic acid (2-Et-IAA)

The reaction and work-up were performed in an efficient fume hood, as highly toxic HCN gas is formed as a by-product. Adapting a method for the synthesis of indole-3-acetic acid (Snyder and Pilgrim 1948), a solution of 2-ethylgramine (1.71 g, 8.46 mmol) and KCN (2.74 g, 42.1 mmol) in 95% ethanol (17.0 mL) and water (3.7 mL) was boiled until TLC (solvents A_5 and B) showed complete consumption of the starting gramine (70 h). After cooling to room temperature, water (3.4 mL) and solid KOH (3.7 g, 65.5 mmol) were added and boiling was resumed for 10 h. The cooled solution was diluted with water (43 mL) and neutral by-products were extracted with diethyl ether. The organic phase was re-partitioned against 5% aq. Na_2CO_3 which was added to the aqueous phase. The latter was then acidified to pH 2.5 with concd HCl and extracted with diethyl ether. Evaporation of the organic phase gave the crude title com-

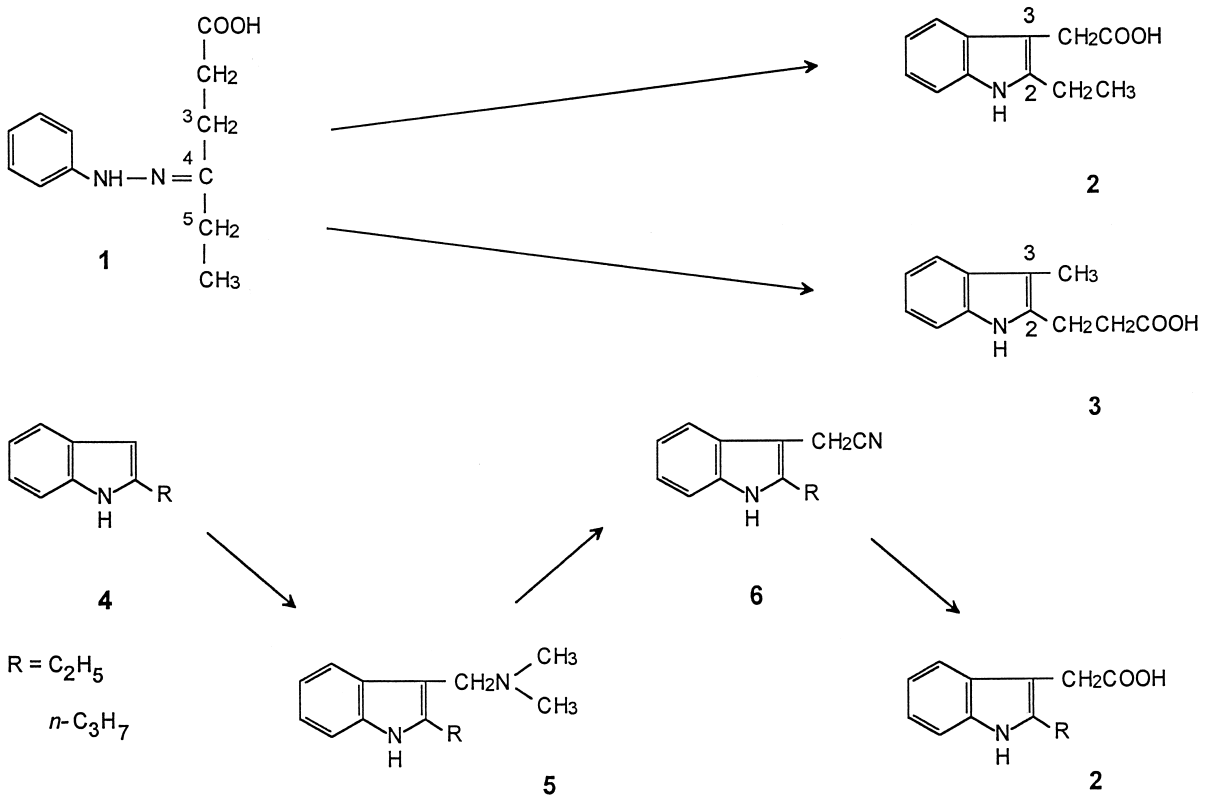

Figure 2. Chemical reactions discussed in the text. The names of the compounds shown are as follows. **1** = 4-phenylhydrazonohexanoic acid, **2** = 2-ethylindole-3-acetic acid (2-Et-IAA), **3** = 3-(3-methylindol-2-yl)propionic acid, **4** = 2-alkylindole, **5** = 2-alkylgramine or *N,N*-dimethyl-(2-alkylindole-3-)methanamine, **6** = 2-alkylindole-3-acetonitrile, **7** = 2-alkylindole-3-acetic acid; 'alkyl' in compounds **4** – **7** is ethyl or *n*-propyl.

pound (1316 mg, 77%). Repeated recrystallization from *1*. ethyl acetate/cyclohexane (20:1) and *2*. chloroform/ethyl acetate (2:1) afforded off-white crystals, m. p. 190–197 °C (decomposition) [lit. (Walton et al. 1968): decomposition at 193–203 °C; crystallization from acetone/petrol]. R_f = 0.5 (solvent A_5), 0.4 (solvent B). *^{1}H-NMR (CD_3OD).* Indole-3-acetic acid moiety: δ7.53 (d, 1H, $J_{4,5}$ = 7.6 Hz, H-4), 7.05 (ddd, 1H, $J_{5,6}$ = 7.0 Hz, $J_{5,7}$ = 1.4 Hz, H-5), 7.11 (ddd, 1H, $J_{4,6}$ = 1.4 Hz, H-6), 7.34 (dd, 1H, $J_{6,7}$ = 7.6 Hz, H-7), 3.75 (s, 2H, CH_2); ethyl moiety: δ2.87 (q, 2H, J_{vic} = 7.6 Hz, CH_2), 1.38 (t, 3H, CH_3). *^{13}C-NMR (CD_3OD).* Indole-3-acetic acid moiety: δ140.3 (C-2), 104.3 (C-3), 130.1 (C-3a), 119.9, 119.0 (C-4, C-6), 121.8 (C-5), 111.7 (C-7), 137.4 (C-7a), 31.1 (CH_2), 176.9 (COOH); ethyl moiety: δ20.5 (α-C), 14.9 (β-C). *UV (95% EtOH).* λ_{max} (log ε) 226.5 (4.47), 276.2 (3.81, shoulder), 283.1 (3.85), 290.4 (3.80); reference values for IAA: 222.7 (4.50), 276.3 (3.73, shoulder), 282.0 (3.76), 290.0 (3.69); 2-Me-IAA: 225.8 (4.44), 276.1 (3.77, shoulder), 282.3 (3.80), 289.8 (3.73). *X-ray structural analysis*. See Figure 3a.

*2-(*n*-Propyl)indole-3-acetic acid (2-Pr-IAA)*

The title compound was prepared from 2-(*n*-propyl)-gramine in essentially the same way as 2-Et-IAA (crude yield: 82%) and repeatedly recrystallized from chloroform to yield off-white crystals, m. p. 150–153 °C [lit. (Rokach 1973): 154–158 °C]. R_f = 0.5 (solvent B), 0.7 (solvent C). *^{1}H-NMR (CD_3OD).* Indole-3-acetic acid moiety: δ7.53 (d, 1H, $J_{4,5}$ = 7.6 Hz, H-4), 7.05 (ddd, 1H, $J_{5,6}$ = 6.6 Hz, $J_{5,7}$ = 1.4 Hz, H-5), 7.11 (dd, 1H, H-6), 7.34 (dd, 1H, $J_{6,7}$ = 7.4 Hz, H-7), 3.75 (s, 2H, CH_2); *n*-propyl moiety: δ2.82 (t, 2H, J_{vic} = 7.5 Hz, α-CH_2), 1.82 (sextet, 2H, β-C), 1.06 (t, 3H, J_{vic} = 7.4 Hz, CH_3). *^{13}C-NMR (CD_3OD).* Indole-3-acetic acid moiety: δ138.8 (C-2), 105.1 (C-3), 130.1 (C-3a), 119.9, 119.1 (C-4, C-6), 121.8 (C-5), 111.7 (C-7), 137.4 (C-7a), 31.2 (CH_2), 176.9 (COOH); *n*-propyl moiety: δ29.3 (α-C), 24.4 (β-C), 14.5 (γ-C). *UV (95% EtOH).* λ_{max} (log ε) 226.4

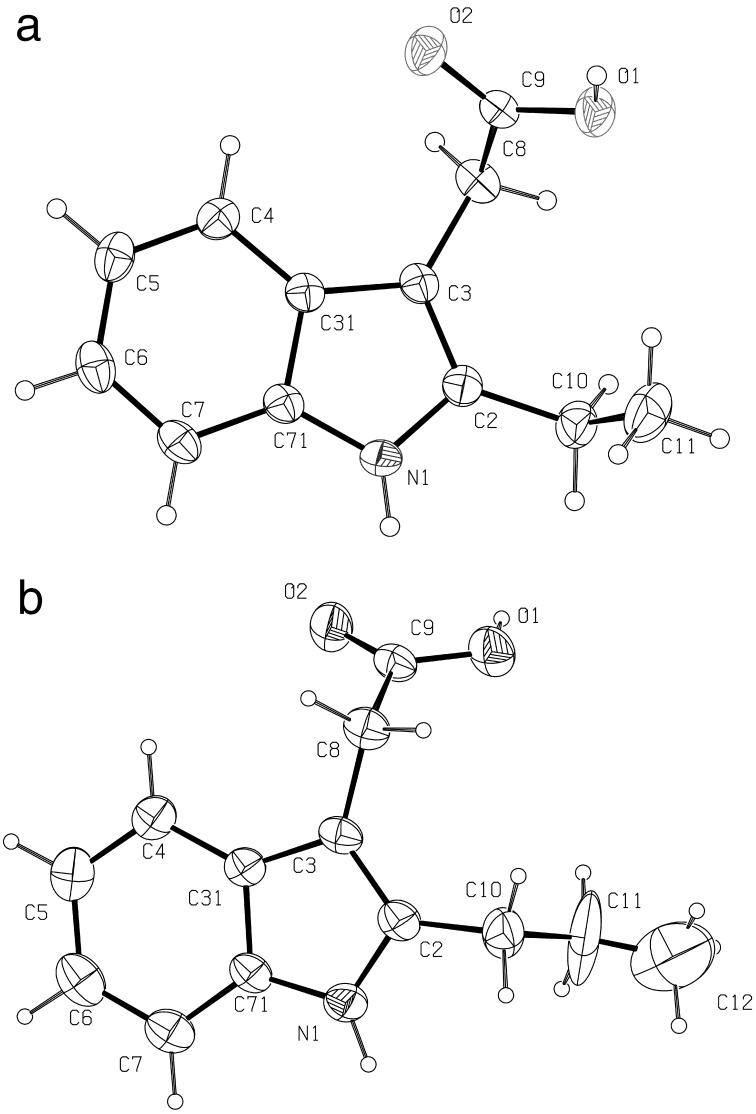

Figure 3. Molecular structures [*ORTEP II* (Johnson 1976)] of (a) 2-ethylindole-3-acetic acid (2-Et-IAA) and (b) 2-(*n*-propyl)indole-3-acetic acid (2-Pr-IAA) showing the crystallographic numbering conventions referred to in the text. The thermal ellipsoids are scaled at the 30% probability level.

(4.49), 276.5 (3.84), 283.1 (3.88), 290.4 (3.82). *X-ray structural analysis*. See Figure 3b.

3-(3-Methylindol-2-yl)propionic acid

4-Phenylhydrazonohexanoic acid was subjected to Fischer cyclization in abs. ethanol/sulfuric acid, as detailed by Kögl and Kostermans (1935) in their attempted synthesis of 2-ethylindole-3-acetic acid. Yield 44% (after one recrystallization from water), m. p. 97–99 °C [The product obtained by Kögl and Kostermans (1935) melted at 100–101 °C]. R_f = 0.5 (solvent B). *^{1}H-NMR ($CDCl_3$).* δ8.05 (broadened s, 1H, H-1), 7.49 (d, 1H, $J_{4,5}$ = 7.8 Hz, H-4), 7.08 (ddd, 1H, $J_{5,6}$ = 6.4 Hz, $J_{5,7}$ = 1.1 Hz, H-5), 7.13 (ddd, 1H, $J_{4,6}$ = 1.4 Hz, H-6), 7.26 (dd, 1H, $J_{6,7}$ = 8.1 Hz, H-7), 2.24 (s, 3H, CH_3), 3.03 (t, 2H, J_{vic} = 6.8 Hz, Ar-CH_2), 2.71 (t, 2H, CH_2COOH). *^{13}C-NMR ($CDCl_3$).* δ133.0 (C-2), 107.4 (C-3), 129.0 (C-3a), 119.0, 118.2 (C-4, C-6), 121.4 (C-5), 110.4 (C-7), 135.2 (C-7a), 8.2 (CH_3), 20.4 (Ar-CH_2), 33.8 (CH_2COOH), 179.4 (COOH). *X-ray structural analysis*. See Figure 4.

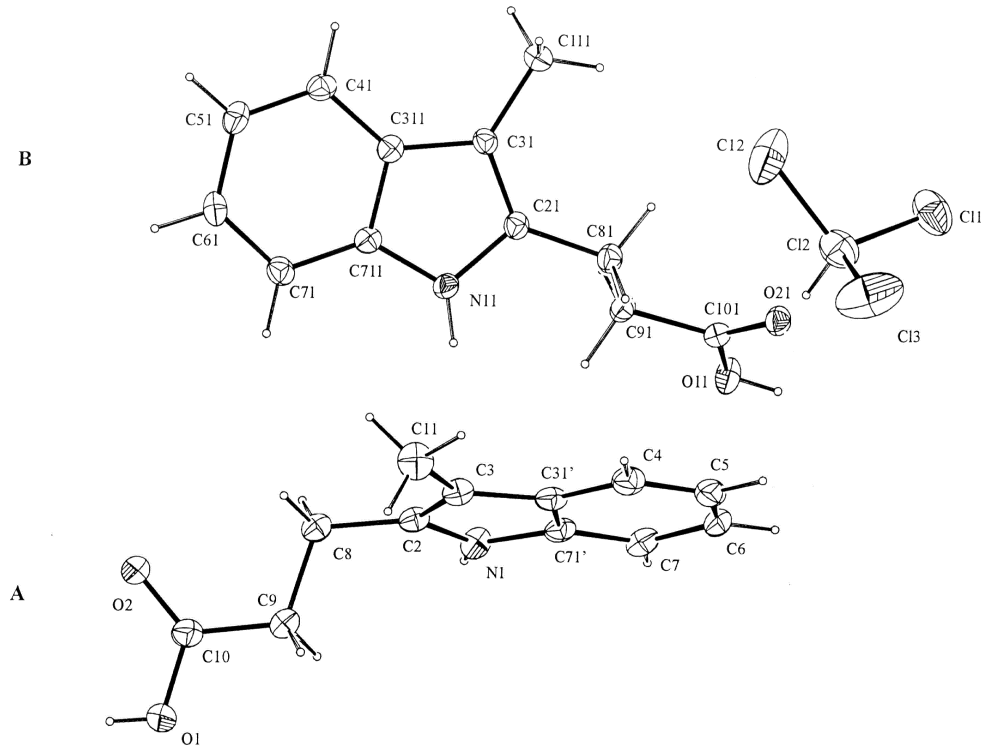

Figure 4. Molecular structure [*ORTEP II* (Johnson 1976)] of 3-(3-methylindol-2-yl)propionic acid. The elementary cell contains two non-equivalent molecules, **A** and **B**, of the indolic acid and a molecule of chloroform, the solvent from which the crystals subjected to X-ray analysis were obtained. Generally, the number '1' was appended to the atom numbers in molecule **B**. Only the two carbons at the junction of the benzene and pyrrole rings required different labeling to avoid confusion: C31′ and C71′ in molecule **A** and C311 and C711 in molecule **B**. The thermal ellipsoids are scaled at the 30% probability level.

X-ray crystallography

Crystals suitable for X-ray structure analysis were prepared by slow evaporation of 2 mL solutions containing 5–10 mg mL^{-1} of compound in $CHCl_3$. The crystals were grown at room temperature overnight. The compounds studied have no chiral centers and accordingly crystallize in the centrosymmetric space groups: $P\bar{1}$ [3-(3-methylindol-2-yl)propionic acid] and $P2_1/a$ (2-Et-IAA and 2-Pr-IAA). Data were collected on an Enraf-Nonius CAD-4 diffractometer (Table 1) with graphite-monochromated Cu$K\alpha$ (2-Et-IAA) and Mo$K\alpha$ (2-Pr-IAA) radiation and rescaled for decay on the basis of intensity reduction of standard reflections. Data for 3-(3-Me-indol-2-yl)propionic acid were exceptionally collected at 133K on a Huber/Stoe diffractometer with attached Siemens Kappa Charge-Coupled Device electronic area detector and using a molybdenum sealed tube. Lorentz and polarization corrections were applied using the *HELENA* (Spek 1993) program. Empirical absorption correction [Ψ-scan, *PLATON* (Spek 1997)] was applied for 2-Et-IAA, and semiempirical from equivalents [*SADABS* (Sheldrick 1996)] for 3-(3-methylindol-2-yl)propionic acid. The structures were solved by the *SHELXS* (Sheldrick 1997a) program and refined using *SHELXL* (Sheldrick 1997b). Hydrogen atoms were generated on stereochemical grounds. The non-H atoms were refined anisotropically; details of the refinement procedures are listed in Table 1. Scattering factors are those included in *SHELXL* (Sheldrick 1997b). Molecular geometry was calculated by the program *PLATON* (Spek 1997). Drawings were prepared using *ORTEPII* (Johnson 1976) incorporated in *PLATON* (Spek 1997). The final atomic coordinates and equivalent isotropic thermal parameters are listed in Tables 2a, 2b, 2c*. Calculations were

* Lists of atomic coordinates, anisotropic displacement parameters and structure factors have been deposited with the IUCr [Reference: CCDC-139864 for 2-Et-IAA and CCDC-139865 for 3-(3-methylindol-2-yl)propionic acid). Copies may be obtained through

performed on a Silicon Graphics *OCTANE* workstation in the Laboratory for Chemical Crystallography and Biocrystallography, Ruđer Bošković Institute, Zagreb, Croatia.

Computational methods

Molecular modeling

Conformational analysis for undissociated 2-alkyl-IAA molecules and the corresponding carboxylate anions was performed by the semiempirical methods PM3 and AM1 from the MOPAC package of programs (Stewart 1990). The conformations (i.e. the corresponding potential-energy surfaces) of 2-Me-IAA and 2-Et-IAA were also, to some extent, analyzed by *ab initio* self-consistent field calculations using the Restricted Hartree-Fock (RHF) formalism and the 6–31G* basis set which was previously found to be adequate for IAA and its ring-substituted derivatives (Ramek et al. 1995, 1996; Ramek and Tomić 1998a, 1998b, 1999). The latter calculations were performed with the program GAMESS (Schmidt et al. 1993). The resulting conformers are grouped into *1. T* (tilted) conformers with the CH_2-COOH bond perpendicular, or near-perpendicular, to the ring plane and *2. P* (planar) conformers with that bond in the ring plane (or nearly so).

To investigate possible conformational transitions of 2-alkyl-IAAs in aqueous solution, molecular dynamics simulations were performed by the program DISCOVER (DISCOVER, release 1997) using the CVFF (Dauber-Osguthorpe et al. 1988) force field and periodic boundary conditions. The optimized conformations were 'soaked' in a cubic box of water with the starting dimensions of 17 × 17 × 17 $Å^3$. Electrostatic interactions were considered up to a distance of 15 Å. The use of two cut-off values utilized together with a smoothing function, for the range of 13.5–15 Å, enabled proper treatment of long distance electrostatic interactions. After equilibrating the system for 10 ps at 300 K, ca. 2 ns of productive simulation was carried out at a temperature ranging from 273–393 K, using 1 fs time steps.

Similarity analysis

The 2-alkyl-IAAs studied herein were compared with three classes of auxin-related compounds: 1) strong auxins, 2) weak auxins with weak antiauxin properties, and 3) inactive compounds with structural relationships to the auxin family. Details of the classification and the mathematical background were described previously (Tomić et al. 1998a, 1998b). In brief, the interaction energies between the 2-alkyl-IAAs and selected 'probes' were calculated for predefined arrays of sampling points, at the molecular surface and at a grid enclosing the molecule. Two of the probes employed reflect general properties of the amino acid residues surrounding the active site of the postulated auxin receptor(s): H_2O for hydrophilic (and thus hydrated under physiological conditions), and DRY for hydrophobic residues. Three further probes conventionally termed NH_2^+, CH_3 and O reflect the interactions with specific functional groups present in many protein amino acids.

P and *T* conformers of auxin molecules required separate treatment. The resulting 'molecular interaction fields' were compared to those obtained for typical representatives of classes 1 to 3. This was accomplished by calculating the Carbó similarity index (Carbó and Calabuig 1992), averaging, if required, over multiple *P* or *T* conformers and over multiple class representatives: the larger the similarity index, the closer the connection to the respective class. The class representatives chosen here were: 4-chloro-2-methylphenoxyacetic acid, IAA and 4-chloro-IAA for class 1, indole-3-propionic acid and 4,7-dichloroindole-3-acetic acid for class 2, and benzoic acid for class 3.

Results and discussion

Growth-promoting properties of 2-Et-IAA and 2-Pr-IAA

2-Et-IAA and 2-Pr-IAA prepared as outlined in the Materials and Methods section were active auxins. Typical dose-response curves are presented in Figure 5. Because of the relatively weak response, bioassays were performed with two oat cultivars and repeated altogether 10 times for 2-Et-IAA and 9 times for 2-Pr-IAA. Dose-dependent growth-promotion was observed in every single case. The results of the experiments in which both alkyl homologues were as-

---

The Managing editor, International Union for Crystallography, 5 Abbey Square, Chester CH1 2HU, England. Due to the high anisotropy of part of the 2-Pr-IAA molecule these data are not deposited.

Table 1. Experimental details for X-ray structure analysis.

Parameter	2-Et-IAA	3-(3-Methylindol-2-yl)propionic acid	2-Pr-IAA
Crystal data			
Chemical formula	$C_{12}H_{13}NO_2$	$C_{12}H_{13}NO_2{\cdot}CHCl_3$	$C_{13}H_{15}NO_2$
Chemical formula weight	203.23	322.60	217.26
Cell setting	monoclinic	triclinic	monoclinic
Space group	$P2_1/a$	$P\bar{1}$	$P2_1/a$
a [Å]	8.7043(2)	9.842(2)	9.154(2)
b [Å]	12.3894(4)	11.053(2)	13.506(2)
c [Å]	9.7720(2)	12.924(3)	9.839(3)
α[degrees]		108.17(3)	
β [degrees]	101.283 (2)	94.41(3)	106.53(2)
γ [degrees]		103.86(3)	
V [Å^3]	1033.46(5)	1279.3(6)	1166.2(5)
D_x [Mg m^{-3}]	1.306	1.365	1.237
Z	4	4	4
Radiation type (wavelength in Å)	CuK_α (1.54184)	MoK_α (0.71073)	MoK_α (0.71073)
μ [mm^{-1}]	0.72	0.35	0.08
F (000)	432	534	464
T [K]	293(2)	133(2)	293(2)
Crystal form	prismatic	prismatic	prismatic
Crystal size [mm]	0.18 × 0.15 × 0.12	0.30 × 0.27 × 0.20	0.17 × 0.13 × 0.19
Crystal color	colorless	colorless	colorless
Data collection			
Diffractometer	Enraf-Nonius CAD-4	Stoe-Siemens-Huber, CCD area detektor	Enraf-Nonius CAD-4
Data collection method	$\omega/2\theta$	phi-scan (resolution 8.129 pixels/mm)	$\omega/2\theta$
Absorption correction	Ψ-scan	semi-empirical (SADABS)	/
No. of measured reflections	2227	4000	2357
No. of observed reflections	1734, $I > 2\sigma(I)$	2932, $I > 2\sigma(I)$	730, $I > 2\sigma(I)$
No. of reflections for cell parameters	25	105	20
θ range [degrees]	40.42–45.43	2–24	22–38
θ max [degrees]	74.3	24	26.3
Range of h, k, l	(−10,10; −15,0; 0,12)	(−11,11; −12,12; 0,14)	(0,11; 0,16; −12,11)
Intensity decay (3 standard reflections measured every 3 h)	<1	<1	<1
Refinement			
Refinement on	F^2	F^2	F^2
R	0.0390, $R(F)$	0.0629, $R(F)$	0.0660, $R(F)$
wR	0.1262, R (on F^2)	0.1692, R (on F^2)	0.2465, R (on F^2)
S	1.006	1.042	0.919
No. of reflections used in refinement	2105	4000	2357
No. of parameters used	138	360	147
Weighting scheme	w = 1/[σ^2 (F_o^2) +(0.0767P)^2+0.18P] where P = (F_o^2+2F_c^2) / 3	w = 1/[σ^2 (F_o^2) +(0.0730P)^2+1.93P] where P = (F_o^2+2F_c^2) / 3	w = 1/[σ^2 (F_o^2) +(0.1155P)^2+0.00P] where P = (F_o^2+2F_c^2) / 3
$(\Delta/\sigma)_{max}$	<0.05	<0.05	<0.05
$(\Delta\rho)_{max}$, $(\Delta\rho)_{min}$ [eÅ^{-3}]	0.20, −0.15	0.62, −0.46	0.23, −0.25

Table 2a. Fractional atomic coordinates and equivalent isotropic displacement parameters (U_{eq}= (1/3) $\Sigma_i\Sigma_j U^{ij}a^i a^j \mathbf{a}_i.\mathbf{a}_j$; in Å^2) for 2-Et-IAA.

Atom	*x*	*y*	*z*	U_{eq}
O1	0.29744(13)	0.01798(11)	1.00399(10)	0.0586(4)
O2	0.41839(13)	–0.03697(11)	0.83763(10)	0.0599(4)
N1	0.00614(14)	0.22382(11)	0.58349(10)	0.0458(4)
C2	0.00693(15)	0.15531(12)	0.69484(10)	0.0426(4)
C3	0.10795(15)	0.07187(11)	0.68679(10)	0.0385(4)
C4	0.27358(16)	0.03014(12)	0.49737(10)	0.0450(4)
C5	0.30446(18)	0.06772(14)	0.37279(10)	0.0518(5)
C6	0.23640(18)	0.16254(15)	0.31237(10)	0.0520(5)
C7	0.13522(17)	0.22231(13)	0.37473(10)	0.0474(4)
C8	0.13982(17)	–0.02324(13)	0.78365(10)	0.0462(5)
C9	0.29675(16)	–0.01422(11)	0.87949(10)	0.0403(4)
C10	–0.09259(19)	0.17843(16)	0.79996(10)	0.0566(5)
C11	–0.0076(3)	0.2359(2)	0.9275(2)	0.0804(8)
C31	0.17047(14)	0.08811(11)	0.56308(10)	0.0372(4)
C71	0.10327(14)	0.18415(12)	0.50015(10)	0.0397(4)

Table 2b. Fractional atomic coordinates and equivalent isotropic displacement parameters (U_{eq}= (1/3) $\Sigma_i\Sigma_j U^{ij}a^i a^j \mathbf{a}_i.\mathbf{a}_j$; in Å^2) for 3-(3-methylindol-2-yl)propionic acid, molecules **A** and **B**

Atom	*x*	*y*	*z*	U_{eq}
Molecule **A**				
O1	–0.0183(4)	–0.3328(3)	0.0635(2)	0.0523(11)
O2	–0.0676(3)	–0.5174(3)	0.1057(2)	0.0427(10)
N1	–0.0691(3)	–0.2040(3)	0.4934(2)	0.0345(11)
C2	–0.1669(4)	–0.3120(3)	0.4159(3)	0.0305(11)
C3	–0.2964(4)	–0.3242(3)	0.4496(3)	0.0319(11)
C4	–0.3703(4)	–0.1798(4)	0.6264(3)	0.0388(14)
C5	–0.3159(5)	–0.0734(4)	0.7222(3)	0.0419(16)
C6	–0.1723(5)	–0.0042(4)	0.7470(3)	0.0413(14)
C7	–0.0791(4)	–0.0391(4)	0.6755(3)	0.0383(14)
C8	–0.1267(4)	–0.3931(4)	0.3137(3)	0.0335(12)
C9	–0.0986(5)	–0.3203(4)	0.2317(3)	0.0434(16)
C10	–0.0611(4)	–0.4004(4)	0.1283(3)	0.0380(12)
C11	–0.4325(4)	–0.4280(4)	0.3887(3)	0.0467(16)
C31	–0.2785(4)	–0.2192(4)	0.5525(3)	0.0321(12)
C71	–0.1350(4)	–0.1469(3)	0.5784(3)	0.0319(12)
Molecule **B**				
O11	0.0949(3)	–0.0870(3)	–0.0970(2)	0.0369(9)
O21	–0.1272(3)	–0.1397(2)	–0.0632(2)	0.0314(8)
N11	–0.1944(3)	–0.5237(3)	–0.4255(2)	0.0274(10)
C21	–0.2178(3)	–0.5191(3)	–0.3198(2)	0.0270(11)
C31	–0.2567(3)	–0.6442(3)	–0.3165(2)	0.0265(11)
C41	–0.2961(4)	–0.8722(3)	–0.4747(3)	0.0309(11)
C51	–0.2925(4)	–0.9261(4)	–0.5849(3)	0.0345(11)
C61	–0.2540(4)	–0.8461(4)	–0.6495(3)	0.0341(12)
C71	–0.2190(4)	–0.7102(4)	–0.6041(3)	0.0310(11)
C81	–0.2019(4)	–0.3883(3)	–0.2317(3)	0.0301(11)
C91	–0.0546(4)	–0.2928(3)	–0.2109(3)	0.0284(11)
C101	–0.0344(4)	–0.1667(3)	–0.1164(3)	0.0276(11)
C111	–0.3006(4)	–0.6860(4)	–0.2213(3)	0.0374(12)
C311	–0.2613(3)	–0.7328(3)	–0.4257(2)	0.0264(11)
C711	–0.2230(3)	–0.6545(3)	–0.4921(2)	0.0265(11)
C*l*1[a]	0.3921(3)	0.1523(3)	–0.1035(2)	0.0683(7)
C*l*2[a]	0.5076(2)	0.3981(2)	0.0722(2)	0.0884(8)
C*l*3[a]	0.6199(2)	0.1799(2)	0.0641(2)	0.1078(9)
C12[a]	0.4663(5)	0.2247(4)	0.0360(3)	0.0561(17)

[a] atoms of chloroform (solvent from which the compound was crystallized) molecules incorporated in the crystal lattice.

sayed in parallel with IAA are summarized in Table 3. The values found for the optimal and half-optimal concentrations of IAA are obviously close to the respective data from a previous, larger, set of experiments (Nigović et al. 2000). The corresponding values for 2-Et-IAA and 2-Pr-IAA were consistently larger (i.e. the negative logarithms shown in Table 3 were smaller) by ca. 0.5 orders of magnitude for the optimal and by ca. 1 order of magnitude for the half-optimal concentrations and, thus, about the same as previously determined for 2-Me-IAA (Nigović et al. 2000). However, the maximal response for 2-Et-IAA and 2-Pr-IAA was only 20–50% of the IAA control, while 2-Me-IAA reached 86% (Nigović et al. 2000). In a similar fashion, increasing chain length of *n*-alkyl substituents at ring position 4, 5, and 6 had little effect on the optimal and half-optimal concentrations, but substantially reduced the maximal response (Nigović et al. 2000).

Chemical syntheses

The synthetic procedures employed are summarized in Figure 2. As shown in its upper part, 4-phenylhydrazonohexanoic acid (**1**) may undergo Fischer cyclization in two ways: either C-3 or C-5 may establish a bond to one of the phenyl *ortho*-position to yield, after elimination of ammonia, 2-Et-IAA (**2**) or 3-(3-methylindol-2-yl)propionic acid (**3**). 2-Et-IAA was allegedly formed using the protocol adopted by Kögl and Kostermans (1935). If this was correct, then the aliphatic region of the ^{1}H-NMR spectrum should show a 2H singlet (CH_2COOH), a 2H quartet (CH_2-CH_3), and a 3H triplet (CH_2-CH_3). The product we obtained repeating the protocol of Kögl and Kostermans (1935) showed, however, a 3H singlet (CH_3) and two 2H triplets (CH_2-CH_2-COOH), the signals expected for 3-(3-methylindole-2-yl)propionic acid.

Table 2c. Fractional atomic coordinates and equivalent isotropic displacement parameters (U_{eq}= (1/3) $\Sigma_i\Sigma_j U^{ij}a^i a^j \mathbf{a}_i.\mathbf{a}_j$; in Å^2) for 2-Pr-IAA.

Atom	*x*	*y*	*z*	U_{eq}
O1	0.2011(4)	0.4948(3)	0.5185(3)	0.0972(16)
O2	0.0727(4)	0.5269(3)	0.6709(3)	0.0942(14)
N1	0.4841(4)	0.2907(3)	0.9357(4)	0.0750(14)
C2	0.4825(5)	0.3605(4)	0.8344(4)	0.0716(17)
C3	0.3808(5)	0.4322(4)	0.8421(4)	0.0647(17)
C4	0.2178(5)	0.4509(4)	1.0192(5)	0.0776(19)
C5	0.1907(6)	0.4078(5)	1.1365(6)	0.092(2)
C6	0.2625(7)	0.3194(5)	1.1910(6)	0.097(3)
C7	0.3623(6)	0.2727(4)	1.1306(5)	0.085(2)
C8	0.3441(5)	0.5243(4)	0.7549(4)	0.0773(19)
C9	0.1931(6)	0.5169(3)	0.6431(5)	0.0695(17)
C10	0.5802(6)	0.3502(5)	0.7392(5)	0.101(3)
C11	0.5108(11)	0.2804(11)	0.6150(8)	0.238(7)
C12	0.5790(14)	0.2562(10)	0.5324(11)	0.269(8)
C31	0.3196(5)	0.4064(4)	0.9563(4)	0.0620(17)
C71	0.3878(5)	0.3172(4)	1.0129(5)	0.0657(19)

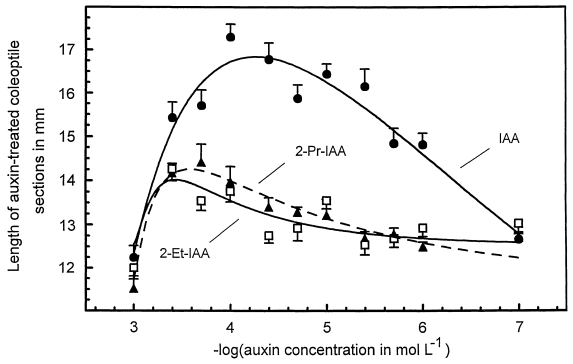

Figure 5. Elongation growth induced by IAA, 2-Et-IAA and 2-Pr-IAA in the *Avena* coleoptile section straight-growth bioassay. The error bars are standard errors of the mean. The data shown are from a single experiment and are intended to illustrate the general shape of the dose-response curves. For quantitative comparisons, the results of a number of experiments were averaged to yield the values shown in Table 3.

The results of X-ray crystallography shown in Figure 4 confirmed that this was indeed the correct structure.

Chandra et al. (1980) allegedly synthesized the proper 2-Et-IAA, as well as 2-Pr-IAA, using a slight modification of the approach of Kögl and Kostermans. Their procedure was, however, not described in sufficient detail and the identity of their products was not documented by error-proof data. Here we prepare 2-Et-IAA (**2**) from the preformed indole ring system (**4**, R = C_2H_5), *via* 2-ethylgramine (**5**, R = C_2H_5) and 2-ethylindole-3-acetonitrile (**6**, R = C_2H_5) (lower part of Figure 2), as reported by Walton et al. (1968) without experimental details. An analogous approach was used to synthesize 2-Pr-IAA, which was previously obtained by catalytic reduction of 2-ethylindolopyrone (Rokach 1973). The lots of 2-Et-IAA and 2-Pr-IAA used in bioassays had melting points consistent with the values given by Walton et al. (1968) and Rokach (1973), while TLC suggested a purity well above 98%. The identity of the 2-alkyl-IAAs was further confirmed by NMR-spectroscopy and X-ray crystallography (Figure 3a, b).

X-ray crystallography

The molecular structures of 2-Et-IAA, 2-Pr-IAA and 3-(3-methylindole-2-yl)propionic acid in the crystalline state were determined by X-ray structure analysis. The results are shown in Figures 3 and 4. Details of the molecular geometry are presented in Tables 4, 5 and 6. Deviations of the molecular geometry of the benzene moiety of the indole ring system, including shortening of the C4-C5 bond (arithmetic mean: 1.375(5) Å; Table 4) and closing of the bond angle C6-C7-C71 (arithmetic mean: 117.4(4)°; Table 5), have already been observed for a large number of other indolic compounds (Nigović et al. (2000) and references cited therein). In the pyrrole ring, alkyl substitution at C2 slightly decreases the endocyclic bond angle at that position, as revealed by comparing the data in Table 5 to the corresponding values for IAA [110.1(2)°] and 2-Me-IAA [108.2(2)°] (Nigović et al. 2000). Comparable changes at the site of substitution were also observed for IAAs alkylated in the benzene moiety (Nigović et al. 2000) indicating adjustments of orbital hybridization due to electronic substituent effects.

The overall conformations of the molecules studied is described by torsion angles (Table 6) C2-C3-C8-C9 (T1) which defines the orientation of the CH_2-COOH group relative to the indole ring plane, and N1-C2-C10-C11 (T3) which reflects the respective orientation of the 2-alkyl substituent. The distal ends of the 2- and 3-substituents are turned to the same side of the ring plane. Both the C8-C9 (CH_2-COOH) and the C10-C11 (CH_2-CH_3 in 2-Et-IAA; CH_2-CH_2 in 2-Pr-IAA) bonds are near-perpendicular to the aromatic system. Moreover, while the carboxyl group in IAA and 2-Me-IAA is coplanar with the C3-C8 bond and thus turned away from C2 (Nigović et al. 2000), the COOH-moiety in 2-Et-IAA and 2-Pr-IAA is ori-

Table 3. Auxin activity of 2-alkylindole-3-acetic acids in the *Avena* coleoptile-section straight-growth test performed with two different oat cultivars.

Compound[a]	Number of assays	Negative logarithm of optimal concentration[b] in mol L^{-1}	Relative optimal elongation[b, c]	Negative logarithm of half-optimal concentration[b] in mol L^{-1}
cv. Valiant				
IAA	4	4.2±0.1	1.00	5.8±0.2
2-Et-IAA	4	3.6±0.1	0.21±0.04	4.6±0.2
2-Pr-IAA	4	3.8±0.1	0.35±0.06	4.9±0.3
cv. Pula				
IAA	4	4.0±0.1	1.00	5.3±0.4
2-Me-IAA[d]	6	3.7±0.1	0.86±0.07	4.7±0.1
2-Et-IAA	4	3.5±0.1	0.40±0.05	4.2±0.2
2-Pr-IAA	4	3.6±0.0	0.49±0.05	4.5±0.2

[a]See Figure 1 for abbreviations. [b]Arithmetic mean ± standard error of the mean. [c]Elongation at optimal concentration *divided by* the elongation at the optimal IAA concentration for the same lot of coleoptiles; elongation = length of auxin-treated coleoptile section *minus* length of coleoptile sections in the water control for the respective lot of coleoptiles. [d]Quoted from Nigović et al. (2000) for comparison. For IAA, in that set of experiments (performed with cv. Pula), the negative logarithm of the optimal concentration was 4.1±0.0 and the negative logarithm of the half-optimal concentration was 5.5±0.1 (n = 15).

Table 4. Bond lengths (Å) for 2-Et-IAA, 3-(3-Me-indol-2-yl)propionic acid and 2-Pr-IAA.

Bond	2-Et-IAA	3-(3-Methylindol-2-yl)propionic acid		2-Pr-IAA
		A[a]	**B**[a]	
N1—C2	1.379(2)	1.382(5)	1.391(5)	1.369(6)
N1—C71	1.374(2)	1.379(5)	1.379(4)	1.365(6)
C2—C3	1.369(2)	1.368(5)	1.359(5)	1.360(6)
C3—C31	1.434(2)	1.432(5)	1.436(5)	1.434(6)
C3—C8	1.503(2)			1.494(6)
C31—C4	1.400(2)	1.407(5)	1.413(5)	1.393(6)
C31—C71	1.413(2)	1.402(5)	1.408(5)	1.397(6)
C4—C5	1.378(2)	1.376(6)	1.369(5)	1.377(7)
C5—C6	1.394(2)	1.394(6)	1.405(5)	1.394(7)
C6—C7	1.380(2)	1.386(6)	1.375(5)	1.376(7)
C7—C71	1.392(2)	1.394(6)	1.394(5)	1.382(6)
C8—C9	1.502(2)	1.523(5)	1.523(5)	1.505(6)
C9—O1	1.279(2)			1.284(5)
C9—O2	1.240(2)			1.217(6)
C2—C8		1.489(5)	1.499(5)	
C2—C10	1.495(2)			1.474(7)
C3—C11		1.506(5)	1.501(5)	
C9—C10		1.483(6)	1.497(5)	
C10—O1		1.316(5)	1.317(4)	
C10—O2		1.218(5)	1.223(4)	
C10—C11	1.499(3)			1.531(1)

[a] **A** and **B** are the two conformers which coexist in the crystalline state. Consult Figure 4 for the numbering of corresponding atoms.

ented in a plane perpendicular to that bond and thus pushes its OH group towards the alkyl chain at the 2-position. These features of the crystal structures indicate that there is no major sterical crowding for the distal ends of the 2- and 3-substituents. For 3-(3-methylindol-2-yl)propionic acid, the positions of C8 (CH_2) and C11 (CH_3) above or below the ring plane are described by torsion angles C31-C3-C2-C8 and C4-C31-C3-C11 (Table 6). The C8-C9 (CH_2-CH_2)

Table 5. Bond angles (degrees) for 2-Et-IAA, 3-(3-methylindol-2-yl)propionic acid and 2-Pr-IAA.

Bond angle	2-Et-IAA	3-(3-Methylindol-2-yl)propionic acid		2-Pr-IAA
		A[a]	B[a]	
C2—N1—C71	109.8(1)	109.4(3)	108.8(3)	110.5(4)
N1—C2—C3	108.9(1)	108.8(3)	109.6(3)	108.4(4)
C2—C3—C8	126.7(1)			127.3(5)
C2—C3—C31	107.2(1)	107.3(3)	107.0(2)	107.3(4)
C31—C3—C8	126.0(1)			125.3(5)
C3—C31—C4	134.3(1)	134.1(4)	134.0(3)	134.7(5)
C3—C31—C71	107.0(1)	107.2(3)	107.3(3)	106.9(4)
C4—C31—C71	118.7(1)	118.7(4)	118.7(3)	118.4(5)
C31—C4—C5	119.0(1)	119.0(4)	118.9(3)	119.5(5)
C4—C5—C6	121.3(1)	121.3(4)	121.5(4)	120.4(6)
C5—C6—C7	121.3(1)	121.3(4)	121.0(3)	121.7(6)
C6—C7—C71	117.5(1)	117.1(4)	117.9(4)	117.0(5)
C31—C71—C7	122.2(1)	122.6(4)	122.1(3)	123.1(5)
N1—C71—C7	130.7(1)	130.1(4)	130.6(3)	129.9(5)
N1—C71—C31	107.1(1)	107.3(3)	107.3(2)	106.9(4)
C3—C8—C9	111.6(1)			111.9(4)
C8—C9—O1	116.8(1)			115.1(5)
C8—C9—O2	120.6(1)			122.1(5)
O1—C9—O2	122.6(1)			122.8(4)
Nl—C2—C10	120.7(1)			121.0(5)
C3—C2—C10	130.5(1)			130.6(5)
Nl—C2—C8		121.6(3)	119.9(3)	
C3—C2—C8		129.5(3)	130.4(3)	
C2—C3—C11		126.2(3)	127.6(3)	
C11—C3—C31		126.6(4)	125.2(3)	
C2—C8—C9		112.5(4)	113.0(3)	
C8—C9—C10		113.3(4)	113.1(3)	
O1—C10—O2		122.9(4)	123.4(3)	
O1—C10—C9		113.7(4)	112.4(3)	
O2—C10—C9		123.4(4)	124.1(3)	
C2—C10—C11	113.8(2)			112.1(5)
C10-C11-C12				122.0(1)

[a] **A** and **B** are the two conformers of 3-(3-methylindol-2-yl)propionic acid which coexist in the crystalline state. Consult Figure 4 for the numbering of corresponding atoms.

bond is near-perpendicular to the ring-plane and approximately coplanar with the COOH group.

Conformational analysis

It has been argued that the conformations adopted by bioactive compounds, in the absence of restraints imposed by the crystal lattice, are more directly related to their biological properties. Under these conditions, a number of conformers coexist; the smaller the conformational strain (energy), the larger the respective subpopulation of conformers, a correlation expressed in quantitative terms by the Boltzmann-Maxwell distribution. As complete conformational analysis by experimental methods is so far not feasible for 2-alkyl-IAAs, we resorted to computational chemistry. Table 7 summarizes the results of conformational analysis performed for isolated molecules of 2-alkyl-IAAs using semiempirical PM3 and *ab initio* Restricted Hartree-Fock/6–31G* calculations. The conformers are described by torsion angles T1 to T4 (consult Table 6 for definitions). For all three compounds, the conformations with the C8-C9 and C10-C11 bonds near-perpendicular to the ring plane have the lowest energies. The global minima for 2-Et-IAA (**C**, **C***) and 2-Pr-IAA (**B**) correspond to conformers

Table 6. Selected torsion angles (°) for 2-Et-IAA, 3-(3-Me-indol-2-yl)propionic acid and 2-Pr-IAA.

Torsion angle	2-Et-IAA	3-(3-Methylindol-2-yl)propionic acid		2-Pr-IAA
		A[a]	**B**[a]	
C2—C3—C8—C9 (T1[b])	−105.9(2)			104.6(6)
C31—C3—C8—C9	78.5(2)			−79.2(6)
C3—C8—C9—O1	100.7(1)			−99.0(5)
C3—C8—C9—O2 (T2[b])	−79.0(2)			77.9(6)
C3—C2—C8—C9		106.8(5)	123.4(4)	
C31—C3—C2—C8		−178.5(4)	177.1(3)	
C2—C8—C9—C10		−178.9(4)	−175.0(3)	
C8—C9—C10—O1		−171.4(4)	177.9(3)	
C8—C9—C10—O2		7.8(6)	−2.5(5)	
C4—C31—C3—C11		0.7(8)	−3.9(6)	
N1—C2—C10—C11 (T3[b])	−96.1(2)			81.3(7)
C2—C10—C11—C12 (T4[b])				−173.8(1)

[a] **A** and **B** are the two conformers which coexist in the crystalline state. Consult Figure 4 for the numbering of corresponding atoms. [b] Labels used in conformational analysis.

with the side chains in the 2- and 3-positions tilted to the same side of the ring-plane. Essentially the same conformation exists in the crystal structures (Table 6), except for the opposite orientation of the carboxyl oxygens (i.e. O1 and O2 interchanged). The latter is due to intermolecular hydrogen bonds in which the carboxyl group participates (data not shown), and reflects the influence of the crystal environment on the molecular conformation. Conformers with the C8-C9 bond in the ring plane have markedly higher energies.

To investigate the behavior of 2-alkyl-IAA molecules in aqueous solution, molecular dynamics simulations were performed. As shown in Figure 6 for the example of 2-Pr-IAA, the population of conformers with both side chains tilted to the indole ring plane was much larger than that of molecules with one of the side chains approximately in that plane. The transitions of the 2-alkyl chain between opposite orientations relative to the ring plane are much more frequent than the corresponding transitions of the 3-CH_2COOH moiety.

IAA and its 2-alkyl derivatives are carboxylic acids with pK values around 4.8, and may thus ionize at physiological pH. However, the pH-equivalent *inside* the active sites of the proteins engaged in auxin perception will remain unknown until these proteins are completely characterized. With respect to this unclear situation, conformational analysis was also performed for the carboxylate ions of 2-alkyl-IAAs using the semiempirical PM3 and AM1 methods. The results obtained by the latter approach (which afforded more consistent results for dissociated molecules) are presented in Table 8, indicating that tilted conformations are lower in energy than their planar rotamers, as they are in the undissociated acids. However, ionization decreases the energy difference between the planar and the tilted conformations, and hence the difference in their abundance under physiological conditions.

Interaction similarity analysis

We previously used interaction similarity analysis to define four classes of auxin-related compounds, including growth inhibitors in addition to the classes defined in the Materials and Methods section (Tomić et al. 1998a, 1998b). As 2-alkyl-IAAs are obviously not inhibitors (at physiological concentrations), here we only investigate how they fit into classes 1–3. For this purpose the representative conformations of the carboxylate ions listed in Table 8 were considered. For each compound, an equal number of *P* and *T* conformations was included. The enhanced flexibility of the 2-alkyl residues, proceeding from 2-Me-IAA to 2-Pr-IAA, was taken into account by considering an increasing number of conformers. For each set of conformers, molecular interaction fields (MIFs) were calculated according to the protocols specified by Tomić et al. (1998a, 1998b), using the probes discussed in the Materials and Methods section.

The interaction similarity indices calculated from the above molecular interaction fields identified the three 2-alkyl-IAAs either as strong (class 1) or as weak (class 2) auxins, depending to some extent on

Table 7. Representative conformations of 2-alkylindole-3-acetic acids characterized by torsion angles T1 (C2-C3-C8-C9), T2 (C3-C8-C9-O2), T3 (N1-C2-C10-C11), T4 (C2-C10-C11-C12) and relative energies (ΔE). The values in the shaded areas were computed by an *ab initio* approach (6-31G*), the other ones by the semiempirical PM3 method. Near-planar (*P*) conformations have T1 ~ 0°, tilted (*T*) conformations T1 ~ 90°, with a margin of ±35°.

Compound	Conformation	Conformational type	T1 degrees	T2 degrees	T3 degrees	T4 degrees	ΔE[a] kcal mol^{-1}
2-Me-IAA	**A**	*T*	85	-79			0
	B	*T*	93	-97			0.3
	C	*P*	4	-92			3.8
	A*	*T*	87	-95			0
	D*	*T*	106	103			0
	E*	*T*	76	-31			3
2-Et-IAA	**A**	*T*	58	-143	-80		1.6
	B	*P*	5	-93	75		3.5
	C	*T*	91	-91	80		0
	D	*T*	82	-37	-72		0.4
	C*	*T*	92	-91	76		0
	D*	*T*	82	-37	-73		1.1
2-Pr-IAA	**A**	*P*	5	-94	75	178	3.5
	B	*T*	91	-91	80	-179	0
	C	*T*	90	-91	79	99	2.5
	D	*T*	82	-36	-73	91	1.9
	E	*T*	83	-37	-72	-180	0.4

The origin of the scale (ΔE = 0) corresponds to the conformation with the lowest energy and is defined separately for each compound and, for 2-Me-IAA and 2-Et-IAA, independently for the data sets obtained by the *ab initio* and semiempirical PM3 approaches.

the specific protocol employed. In each case was 2-Me-IAA somewhat better (about 10% larger differences for similarity indices) distinguished from class 3 (inactive compounds) than 2-Et-IAA and 2-Pr-IAA, as demonstrated by the examples presented in Table 9. This is in general accord with the results of the bioassays: 2-Me-IAA is at the borderline between strong and weak auxins; 2-Et-IAA and 2-Pr-IAA are about as 'active' as 2-Me-IAA if half-optimal concentrations are considered, but the maximal response is only about one-half that for 2-Me-IAA (Table 3, cv. Pula).

Concluding remarks

Kögl and Kostermans (1935) attempted the synthesis of 2-Et-IAA by an ambiguous method and could not, at that time, easily verify the structure of their product. Repeating their protocol, we obtained a compound of about the same melting point, but NMR spectra and X-ray data revealed a different identity: 3-(3-methylindol-2-yl)propionic acid. It is not surprising that this compound is inactive in the *Avena* curvature test (Kögl and Kostermans 1935), because the auxin activity of indole-2-acetic acid in the same bioassay is also 'a lot smaller' (Schindler 1958) than that of its positional isomer, IAA. The authentic 2-Et-IAA and its homologue, 2-Pr-IAA show definite auxin activity.

Like any hormone, auxins must interact with specific cell proteins to trigger a biological response. In spite of much effort, and some initial success (McDonald 1997; Woo et al. 2002), the complete set of these proteins has not yet been characterized. According to Katekar's (1979) model of the idealized auxin-

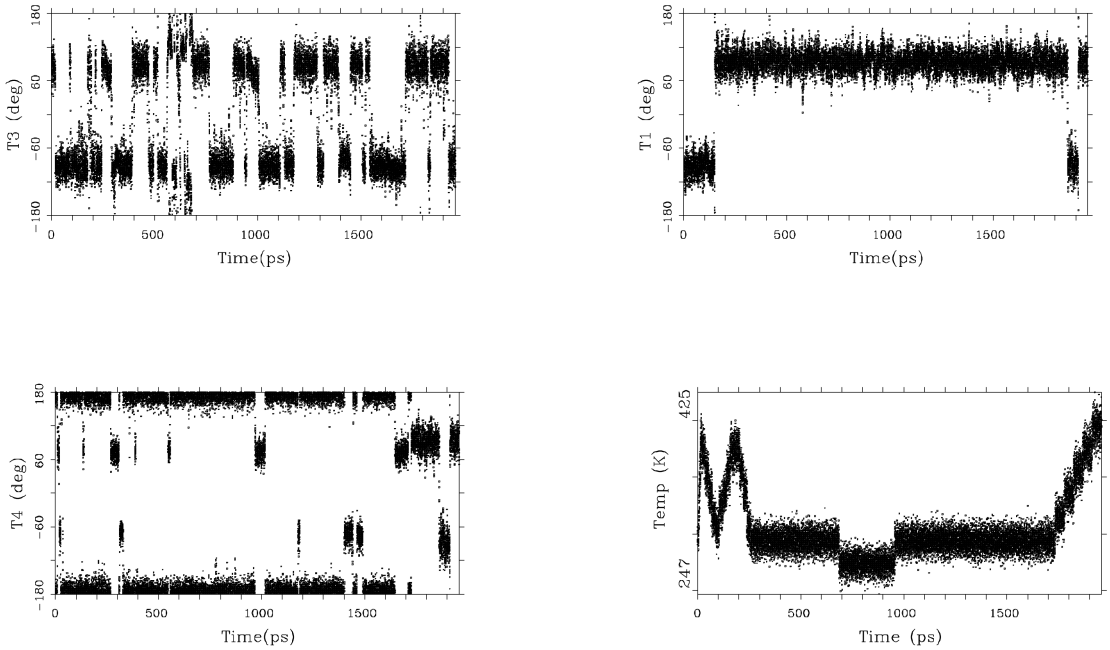

Figure 6. Molecular dynamics simulations for 2-(*n*-propyl)indole-3-acetic acid (2-Pr-IAA) in aqueous solution. Presented are the temperature regime and the changes of torsion angles T1, T3 and T4 within a time interval of 2 nanoseconds.

Table 8. Representative, AM1-optimized conformations of the *carboxylate anions* of 2-alkylindole-3-acetic acids characterized by torsion angles T1 (C2—C3—C8—C9), T3 (N1—C2—C10—C11), T4 (C2—C10—C11—C12) and relative energies (ΔE). The torsion angle T2 cannot be unambiguously defined because the two oxygen atoms in the resonance-stabilized carboxylate ion are equivalent. Near-planar (*P*) conformations have T1 ∼ 0°, tilted (*T*) conformations have T1 ∼ 90°, with a margin of ±25°.

Compound	Conformation	Conformational type	T1 degrees	T3 degrees	T4 degrees	ΔE[a] kcal mol^{-1}
2-Me-IAA	**A**	*P*	6			2.1
	B	*T*	70			0
2-Et-IAA	**A**	*P*	20	−7		0
	B	*P*	4	78		1.2
	C	*T*	99	81		0.6
	D	*T*	100	−82		1.2
2-Pr-IAA	**A**	*P*	2	−6	−179	0.5
	B	*P*	2	−11	83	1.6
	C	*P*	4	94	−67	1.7
	D	*P*	1	86	−175	0.9
	E	*T*	102	106	−179	0
	F	*T*	101	105	−75	0.7
	G	*T*	88	−82	180	1.5
	H	*T*	78	−90	75	1

[a] The origin of the scale (ΔE = 0) corresponds to the conformation with the lowest energy (global minimum) and is defined separately for each compound.

binding site, the acidic head group and the planar body of an auxin are recognized by separate sections of a polypeptide chain which engulfs the target molecule. According to our X-ray data for 2-Me-IAA (Nigović et al. 2000), 2-Et-IAA and 2-Pr-IAA (this paper), neither the indole nucleus nor the CH_2COOH group, considered separately, show structural features which are not encountered in other, more active, indole auxins. Also, the molecular structures in the solid state provide no indications for major sterical crowding involving the 3-CH_2COOH and 2-alkyl groups. However, when not exposed to crystal packing forces,

Table 9. Typical examples for the differences between mean similarity indices relating 2-alkylindole-3-acetic acids to auxin classes 1 (highly active) and 3 (inactive) using the 'probes' listed.

Set of molecular interaction fields	Compound	Probe[c]				
		H_2O	NH_2^+	CH_3	O	DRY
A[a]	2-Me-IAA	0.150	0.064	0.142	0.055	0.341
	2-Et-IAA	0.139	0.063	0.124	0.048	0.341
	2-Pr-IAA	0.138	0.062	0.128	0.048	0.369
B[b]	2-Me-IAA	0.136	0.118	0.118	0.123	0.295
	2-Et-IAA	0.132	0.118	0.119	0.117	0.252
	2-Pr-IAA	0.123	0.116	0.110	0.108	0.189

[a] *P* conformers aligned by the program SEAL (.) [b] *T* conformers aligned by optimizing molecular interaction fields at the molecular surface. [c] represent relevant functional groups (NH_2^+, CH_3, O), as well as hydrophilic (H_2O) and hydrophobic (DRY) elements in the polypeptide chain which engulfs the auxin-binding site in the putative auxin receptor(s).

2-alkyl-IAAs appear to have distinct conformational preferences. Thus, conformational analysis for isolated molecules and molecular dynamics simulations in aqueous solution strongly suggest that alkyl substitution at the 2-position 'pushes' the -CH_2COOH group into conformations with T1 $\sim$ 90° ('*T*-conformations'). Planar (*P*) conformations (T1 $\sim$ 0°), on the other hand, which are preferred by most other indole auxins which have so far been subjected to detailed conformational analysis (Ramek et al. 1996; Ramek and Tomić 1998a, 1998b, 1999), are significantly less populated for undissociated 2-alkyl-IAAs, becoming somewhat more abundant when the carboxyl group ionizes. These conformational preferences in solution (i.e. *before* entering the active site of an auxin-binding protein) would affect the energy input needed to give the 3-side chain the right twist to make both the carboxyl group and the indole ring snap into their optimal positions in their respective compartments of the auxin-binding site. Half-optimal concentrations in auxin bioassays have been interpreted as the dissociation constants (K_d) of the auxin-receptor complexes involved in the biological response (Libbenga et al. 1986). In accord with this view, it follows from the data presented in Table 3 that the binding energy (-ΔG) of IAA (calculated as $\Delta G = RT\ln K_d$; T = 298 K) is 0.8 to 1.5 kcal mol^{-1} more negative than for its 2-alkyl derivatives (note that *more negative* binding energy means *stronger* binding). This is indeed within the energy range required for interconversion of the more abundant conformations of 2-alkyl-IAAs (Tables 8 and 9), and the energy spent on such adjustments would reduce the net binding energy. An energy of 0.8 to 1.5 kcal/mol would also be sufficient for slight displacement of the polypeptide chain around the indole-binding compartment to create space for the 2-alkyl group. However, if this should be the necessary, it would be difficult to understand why 2-Et-IAA and 2-Pr-IAA have about the same half-optimal concentrations, and hence about the same net binding energies, as 2-Me-IAA, even though the size of the 2-alkyl groups varies within wide limits.

On the other hand, IAA and its 2-alkyl derivatives differ considerably with respect to the growth response they elicit at their optimal concentrations, a phenomenon for which Katekar (1979) introduced the term 'efficacy'. This effect could be rationalized by assuming that bulky substituents in the IAA 2-position prevent the auxin-loaded receptor from assuming the conformation which is optimal for initiating a growth response. However, the following kinetic explanation appears at least as likely. To avoid a never-ending growth-stimulating effect of an auxin-loaded 'receptor' protein, there must be ways of disposing of it (by metabolism, forced unloading in the next step of the signal transduction sequence etc.). The rate at which this occurs, relative to the rate of formation of the auxin-protein complex, would determine its stationary concentration, which would translate into the growth rate. The 'induced fit' of an auxin molecule to an auxin-binding site, in the above sense, is accomplished by random conformational changes (through thermal movement) and selection for optimal (largest free-energy gain) protein-ligand interactions, a process which takes time. As 2-alkyl-IAAs have different conformational preferences than IAA, it is plausible to expect that they accommodate themselves more slowly in a binding site nature designed for IAA, and the stationary concentration of the auxin-receptor complex should decrease accordingly. Indeed, the 'maximal response' for 2-Me-IAA is only

about 85% of the value found for IAA in the same lot of *Avena* coleoptiles (Nigović et al. 2000). For 2-Et-IAA and 2-Pr-IAA, additional time should be required for the tail of the 2-substituent (mobility confirmed by molecular dynamics simulations) to assume a conformation which does not interfere with simultaneous binding of the indole nucleus and the carboxyl group. As expected, the maximal response for the latter two auxins reaches only 20–50% of the value obtained for IAA. In a similar fashion, alkylation of IAA at the benzene ring does not markedly affect their half-optimal concentrations, but efficacy drops as the length of the alkyl chain increases (Nigović et al. 2000).

It has been argued that differences in auxin activity can also be due to differences in metabolic stability. This possibility must always be borne in mind, even though there is little, if any, unequivocal supporting evidence. IAA is preferentially metabolized by oxidation at the 2-position which occurs either directly (Ernstsen et al. 1987; Klämbt 1959; Reinecke and Bandurski 1983) or following conjugation with aspartic or glutamic acids (Catalá et al. 1992; Plüss et al. 1989; Östin et al. 1992, 1995, 1998; Riov and Bangerth 1992; Tsurumi and Wada 1986a, 1986b; Tuominen et al. 1994). The compounds studied here cannot be oxidized at the 2-position which is blocked by an alkyl substituent. It is thus unlikely that 2-alkyl-IAAs are metabolized faster than the unsubstituted parent compound.

Acknowledgements

Supported by grants no. 00980608 and 00981010 by the Ministry of Science and Technology of the Republic of Croatia and by US-Croatian Research Agreement JF202. We are grateful to Vladislav Tomišić for recording the UV spectra.

References

Antolić S., Kojić-Prodić B., Tomić S., Nigović B., Magnus V. and Cohen J.D. 1996. Structural studies on monofluorinated derivatives of the phytohormone indole-3-acetic acid (auxin). Acta Crystallogr., Sect. B: Struct. Sci. 52: 651–661.

Antolić S., Salopek B., Kojić-Prodić B., Magnus V. and Cohen J.D. 1999. Structural characterization and auxin properties of dichlorinated indole-3-acetic acids. Plant Growth Regul. 27: 21–31.

Carbó R. and Calabuig B. 1992. Molecular quantum similarity measures and *n*-dimensional representation of quantum objects. I. Theoretical foundations. Int. J. Quant. Chem. 42: 1681–1693.

Catalá C., Östin A., Chamarro J., Sandberg G. and Crozier A. 1992. Metabolism of indole-3-acetic acid by pericarp discs from immature and mature tomato (*Lycopersicon esculentum* Mill.). Plant Physiol. 100: 1457–1463.

Chandra U., Gupta A.A. and Sengupta A.K. 1980. Studies on potential juvenile hormone analogs: part I – Synthesis & physical studies of some heterocyclic geranyl & citronellyl ethers, their epoxides, hydrochlorides & bromides. Indian J. Chem., Sect B: Org. Chem. Incl. Med. Chem. 19: 528–531.

Cosgrove D.J. 1998. Cell wall loosening by expansins. Plant Physiol. 118: 333–339.

Dauber-Osguthorpe P., Roberts V.A., Osguthorpe D.J., Wolff J., Genest M. and Hagler A.T. 1988. Structure and energetics of ligand binding to proteins: *Escherichia coli* difolate reductase-trimethoprim, a drug-receptor system. Proteins: Struct., Funct., Genet. 4: 31–47.

DISCOVER, release 1997. Molecular Simulations, Inc., San Diego, CA, USA.

Ernstsen A., Sandberg G. and Lundström K. 1987. Identification of oxindole-3-acetic acid, and metabolic conversion of indole-3-acetic acid to oxindole-3-acetic acid in seeds of *Pinus sylvestris*. Planta 172: 47–52.

Hatano T., Katayama M. and Marumo S. 1987. 5,6-Dichloroindole-3-acetic acid as a potent auxin: its synthesis and biological activity. Experientia 43: 1237–1239.

Hoffmann O.L., Fox S.W. and Bullock M.W. 1952. Auxin-like activity of systematically substituted indoleacetic acids. J. Biol. Chem. 196: 437–441.

Johnson C.K. 1976. *ORTEPII*. Report ORNL – 5138. Oak Ridge National Laboratory, Tennessee, USA.

Jönsson L. 1961. Chemical structure and growth activity of auxins and antiauxins. In: Ruhland W. (ed.), Encyclopedia of Plant Physiology. Vol. 14. Springer-Verlag, Berlin, pp. 958–1006.

Katayama M., Kato Y., Hatano T., Hatori M. and Marumo S. 1998. Synthesis and biological activities of 5,6-difluoroindole-3-acetic acid; a new fluoroindole auxin. J. Pesticide Sci. 23: 289–295.

Katekar G.F. 1979. Auxins: on the nature of the receptor site and molecular requirements for auxin activity. Phytochemistry 18: 223–233.

Kearsley S.K. and Smith G.M. 1990. SEAL. Tetrahedron Computer Methodol. 3: 615.

Klämbt H.D. 1959. Die 2-Hydroxy-indol-3-essigsäure, ein pflanzliches Indolderivat. Naturwissenschaften 46: 649.

Kloetzel M.C. 1948. Reactions of nitroparaffins. II. Addition of nitroparaffins to unsaturated esters. J. Am. Chem. Soc. 70: 3571–3576.

Kögl F. and Kostermans D.G.F.R. 1935. Über die Konstitutions-Spezifizität des Hetero-auxins. Hoppe Seyler's Z. physiol. Chem. 235: 201–216.

Kojić-Prodić B., Nigović B., Tomić S., Ilić N., Magnus V., Giba Z. et al. 1991. Structural studies on 5-(*n*-alkyl)-substituted derivatives of the plant hormone indole-3-acetic acid. Acta Crystallogr., Sect. B: Struct. Sci. 47: 1010–1019.

Larsen P. 1961. Biological determination of natural auxin. In: Ruhland W. (ed.), Encyclopedia of Plant Physiology. Vol. 14. Springer-Verlag, Berlin, pp. 521–582.

Lawson W.B., Patchornik A. and Witkop B. 1960. Substitution, oxidation and group participation in the bromination of indoles. J. Am. Chem. Soc. 82: 5918–5923.

Le Goffic F., Gouyette A. and Ahoud A. 1973. Une nouvelle synthèse de l'ellipticine et ses analogues structuraux. Tetrahedron 29: 3357–3362.

Libbenga K.R., Maan A.C., van der Linde P.C.G. and Mennes A.M. 1986. Auxin receptors. In: Chadwick C.M. and Garrod D.R. (eds), Hormones, Receptors and Cellular Interactions in Plants. Cambridge University Press, Cambridge, UK, pp. 1–68.

McDonald H. 1997. Auxin perception and signal transduction. Physiol. Plant. 100: 423–430.

Mitchell J.W. and Livingston G.A. 1968. Methods of studying plant hormones and growth-regulating substances. Agriculture Handbook No. 336. Agricultural Research Service, United States Department of Agriculture, Washington, DC, USA.

Muir R.M. and Hansch C. 1953. On the mechanism of action of growth regulators. Plant Physiol. 28: 218–232.

Muir R.M., Hansch C.H. and Gallup A.H. 1949. Growth regulation by organic compounds. Plant Physiol. 24: 359–366.

Nigović B., Antolić S., Kojić-Prodić B., Kiralj R., Magnus V. and Salopek-Sondi B. 2000. Correlation of structural and physicochemical parameters with the bioactivity of alkylated derivatives of indole-3-acetic acid, a phytohormone (auxin). Acta Crystallogr., Sect. B: Struct. Sci. 56: 94–111.

Östin A., Catalá C., Chamarro J. and Sandberg G. 1995. Identification of glucopyranosyl-β-4,1-glucopyranosyl-β-1-*N*-oxindole-3-acetyl-*N*-aspartic acid, a new IAA-catabolite, with liquid chromatography-tandem mass spectroscopy. J. Mass Spectrom. 30: 1007–1017.

Östin A., Kowalczyk M., Bhalerao R.P. and Sandberg G. 1998. Metabolism of indole-3-acetic acid in Arabidopsis. Plant Physiol. 118: 285–296.

Östin A., Monteiro A.M., Crozier A., Jensen E. and Sandberg G. 1992. Analysis of indole-3-acetic acid metabolites from *Dalbergia dolichopetala* by high performance liquid chromatography-mass spectrometry. Plant Physiol.: 63–68.

Plüss R., Jenny T. and Meier H. 1989. IAA-induced adventitious root formation in greenwood cuttings of *Populus tremula* and formation of 2-indolone-3-acetylaspartic acid, a new metabolite of exogenously supplied indole-3-acetic acid. Physiol. Plant. 75: 89–96.

Porter W.L. and Thimann K.V. 1965. Molecular requirements for auxin action – I. Halogenated indoles and indoleacetic acids. Phytochemistry 4: 229–243.

Ramek M., Tomić S. and Kojić-Prodić B. 1995. Systematic ab initio SCF conformational analysis of indol-3-ylacetic acid phytohormone (auxin): comparison with experiment and molecular mechanics calculations. Int. J. Quantum Chem.: Quantum Biol. Symp. 22: 75–81.

Ramek M.L., Tomić S. and Kojić-Prodić B. 1996. Comparative ab initio SCF conformational study of 4-chloro-indole-3-acetic acid and indole-3-acetic acid phytohormones (auxins). Int. J. Quantum Chem. 60: Quantum Biol. Symp. 23: 3–9.

Ramek M. and Tomić S. 1998a. RHF conformational analysis of the auxin phytohormones *n*-ethyl-indole-3-acetic acid (n = 4, 5, 6). Int. J. Quantum Chem. 70: 1169–1175.

Ramek M. and Tomić S. 1998b. Ab initio RHF investigation of mono- and dichlorinated indole-3-acetic acid (IAA) phytohormones. J. Mol. Struct. (Theochem.) 454: 167–173.

Ramek M. and Tomić S. 1999. Quantum chemical conformational analysis of the auxin phytohormone 4-methyl-3-indoleacetic acid. Int. J. Quantum Chem. 75: 1003–1008.

Reinecke D.M. and Bandurski R.S. 1983. Oxindole-3-acetic acid, an indole-3-acetic acid catabolite in *Zea*. Plant Physiol. 71: 211–213.

Rescher U., Walther A., Schiebl C. and Klämbt D. 1996. *In vitro* binding affinities of 4-chloro-, 2-methyl-, 4-methyl, and 4-ethylindoleacetic acid to auxin-binding protein 1 (ABP1) correlate with their growth-stimulating activities. J. Plant Growth Regul. 15: 1–3.

Riov J. and Bangerth F. 1992. Metabolism of auxin in tomato fruit tissue. Formation of high molecular weight conjugates of oxindole-3-acetic acid via the oxidation of indole-3-acetylaspartic acid. Plant Physiol. 100: 1396–1402.

Rokach J. 1973. Indole derivatives. Canadian Patent 926410.

Schindler W. 1958. Indol-2-essigsäure. Helv. Chim. Acta 41: 1441–1443.

Schmidt M.W., Baldridge K.K., Boatz J.A., Elbert S.T., Gordon M.S., Jensen J.H. et al. 1993. General atomic and molecular electronic structure systems. J. Comput. Chem. 14: 1347–1363.

Sell H.M., Wittwer S.H., Rebstock T.L. and Redemann C.T. 1952. Comparative stimulation of parthenocarpy in the tomato by various indole compounds. Plant Physiol. 28: 481–487.

Sheldrick G.M. 1996. *SADABS* program for absorption correction. University of Göttingen, Göttingen, Germany.

Sheldrick G.M. 1997a. SHELXS-97. Program for crystal structure solution. University of Göttingen, Göttingen, Germany.

Sheldrick G.M. 1997b. SHELXL97. Program for crystal structure refinement. University of Göttingen, Göttingen, Germany.

Snyder H.R. and Pilgrim F.J. 1948. The preparation of 3-indoleacetic acid; a new synthesis of tryptophol. J. Am. Chem. Soc.: 3770–3771.

Spek A.L. 1993. *HELENA* program for data reduction. University of Utrecht, Utrecht, The Netherlands.

Spek A.L. 1997. PLATON. Molecular geometry program. Version of 1997. University of Utrecht, Utrecht, The Netherlands.

Stewart J.J.P. 1990. MOPAC 6.0, available from Quantum Chemistry Program Exchange. Indiana University, Bloomington, Indiana, USA.

Tomić S., Gabdoulline R.R., Kojić-Prodić B. and Wade R.C. 1998a. Classification of auxin plant hormones by interaction property similarity indices. J. Computer-Aided Mol. Design 12: 63–79.

Tomić S., Gabdoulline R.R., Kojić-Prodić B. and Wade R. 1998b. Classification of auxin related compounds based on similarity of their interaction fields: Extension to a new set of compounds. Internet J. Chem. 1: 26.

Tsurumi S. and Wada S. 1986a. Identification of 3-hydroxy-2-indolinone-3-acetylaspartic acid as a new indole-3-acetic acid metabolite in *Vicia* roots. Plant Cell Physiol. 27: 559–562.

Tsurumi S. and Wada S. 1986b. Dioxindole-3-acetic acid conjugates formation from indole-3-acetylaspartic acid in *Vicia* seedlings. Plant Cell Physiol. 27: 1513–1522.

Tuominen H., Östin A., Sandberg G. and Sundberg B. 1994. A novel metabolic pathway for indole-3-acetic acid in apical shoots of *Populus tremula* (L.) × *Populus tremuloides* (Michx.). Plant Physiol. 106: 1511–1520.

Verley M.A. and Beduwé J. 1925. Méthode générale de préparation des dérivés substitués de l'indole. Bull. Soc. Chim. France 37: 189–191.

Walton E., Jenkins S.R., Nutt R.F. and Holly F.W. 1968. Some analogs of 1-*p*-chlorobenzyl-5-methylindole-3-acetic acid. J. Med. Chem. 11: 1252–1255.

Woo E.-J., Marshall J., Bauly J., Chen J.-G., Venis M., Napier R.M. et al. 2002. Crystal structure of auxin-binding protein 1 in complex with auxin. EMBO J. 21: 2877–2885.